International Journal of Recent Technology and Engineering (IJRTE)
ISSN: 2277-3878 (Online), Volume-8 Issue-4, November 2019

Self-Calibration of Ultrasonic Water Flow Meter

Muammer Catak, Coskun Ergan

Abstract*: Due to fluid properties, flow patterns, external factors (temperature, pressure, etc.) measurement shows a dynamical characteristic. Therefore, calibration is an indispensable process in order to ensure the standards of flow metering. Ultrasonic flow meters, which are ameliorated the readings over time, are promising devices to minimize the flow measurements error. In this paper, the calibration procedure of a specific ultrasonic water flow meter is discussed, and then a wireless system is proposed to carry out fine calibration. According to the results, piecewise linear least squares approach supplies the best performance at overall volumetric flow rates accompanying with wireless fine calibration system based on RF communication

Keywords*: Calibration; measurement; regression; ultrasonic flow meter; RF communication

I. INTRODUCTION

Ultrasound-based technology has been applied in science and engineering area such as biomedical image processing, target detection, measurement of fluid flow [1]. Motion of ultrasound wave through the media; similarities and discrepancies of the transmitted and the received ultrasonic signals; and their some characteristics have commonly been observed in order to analyze and understand behaviors of the system under investigation. The commonly used ultrasonic flow meter configuration is depicted in Fig. 1. Due to fluid properties, flow patterns, external factors (temperature, pressure, etc.) measurement shows a dynamical characteristic. Hence, calibration is an inevitable procedure for the ultrasonic flow meters [2-6]. It is simply a comparison between the readings and the standards of a flow meter. Obviously, there should be a confidence interval in which the measurement is accepted as valid. Linearity, repeatability, reproducibility, traceability, and stability are significant phenomenon such that a calibrated flow meter fulfills as precise as measurements within an acceptable error band [7-10].

Manuscript published on November 30, 2019.
* Correspondence Author
Muammer Catak*, College of Engineering and Technology, American University of the Middle East, Kuwait. Email: Muammer.Catak@aum.edu.kw
Coskun Ergan, Baylan Measurement Instruments, Izmir, Turkey. Email: c.ergan@baylanwatermeter.com

The formal definition of the calibration is "operation that, under specified conditions, in a first step, establishes a relation between the quantity values with measurement uncertainties provided by measurement standards and corresponding indications with associated measurement uncertainties and, in a second step, uses this information to establish a relation for obtaining a measurement result from an indication." [11]. Calibration can be divided into two stages. Primary standard calibration is based on measurements of physical variables as mass, volume, and time. Secondary standard calibration consists of calibrating a flow meter against another calibrated flow meter.

In this paper, the practical applications of calibration procedure for the massive productions and specific fine calibration via RF signals have been discussed for the case of ultrasonic flow meter. The rest of the paper is organized as follows: In Section 1 calculation of volumetric flow rate of ultrasonic flow meters were discussed in details. In Section 2, commonly used calibration techniques were examined. Specifically purposed fine calibration by means of RF communication is proposed in Section 3. The results are depicted a discussed in Section 4. Finally, the paper is concluded in Section 5.

II. MATERIALS AND METHODS

A. Calculation of Volumetric Flow Rates

The time-of-flight (ToF) is simply defined as the duration in which an ultrasonic signal travels through a medium to a target [12,13]. Considering the configuration with mirrors, the downstream ToF, t_1, and the upstream ToF, t_2, defined as;

$$\begin{aligned} t_1 &= \frac{2d}{c} + \frac{L}{c+v} \\ t_2 &= \frac{2d}{c} + \frac{L}{c-v} \end{aligned} \quad (1)$$

where c is the ultrasound speed in water, and v is the flow velocity.

The difference between upstream and downstream ToFs, Δt is;

$$\Delta t = t_2 - t_1 = \frac{L}{c-v} - \frac{L}{c+v} = \frac{2Lv}{c^2-v^2} \quad (2)$$

while,

$$t_1 t_2 = \left(\frac{2d}{c} + \frac{L}{c+v}\right)\left(\frac{2d}{c} + \frac{L}{c-v}\right) \quad (3)$$

After algebraic manipulations one can easily derived that,

$$t_1 t_2 = \frac{4d^2}{c^2} + \frac{4Ld+L^2}{c^2-v^2} \quad \text{and} \quad c^2 - v^2 = \frac{4Ld+L^2}{t_1 t_2 - \frac{4d^2}{c^2}} \tag{4}$$

By invoking (4) into (2), the flow velocity can be expressed as;

$$v = \frac{\Delta t}{2L}(c^2 - v^2) = \frac{\Delta t}{2L}\frac{4Ld+L^2}{t_1 t_2 - \frac{4d^2}{c^2}} = \frac{4d+L}{2}\frac{\Delta t}{t_1 t_2 - \frac{4d^2}{c^2}} = K\frac{\Delta t}{t_1 t_2 - \frac{4d^2}{c^2}} \tag{5}$$

In literature, since d is in mm range, and c is circa $1500\,\mathrm{m/s}$ regarding to SI units, $4d^2/c^2$ term in the denominator is ignored.

Thereafter, (5) turns into,

$$v = K\frac{\Delta t}{t_1 t_2} \tag{6}$$

Although, $4d^2/c^2$ term is around 10^{-10} range that does not mean to be ignorable since $t_1 t_2$ is roughly between 10^{-10} and 10^{-9}, therefore, using (6) instead of (5) results in errors that has to be diminished during calibration process. The author suggests using an appropriate constant instead of neglecting of the term $4d^2/c^2$.

After determining the flow velocity, the volumetric flow rate, Q is calculated as;

$$Q = Av = \mathcal{K}\frac{\Delta t}{t_1 t_2 - \frac{4d^2}{c^2}} \tag{7}$$

where A is the cross sectional area of the pipe.

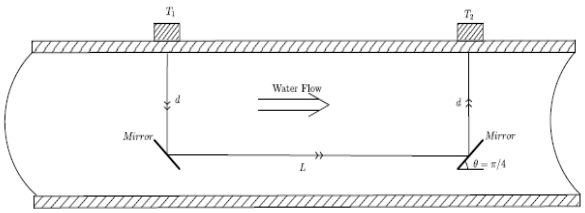

Fig.1. Ultrasonic flow meter with 45° mirrors

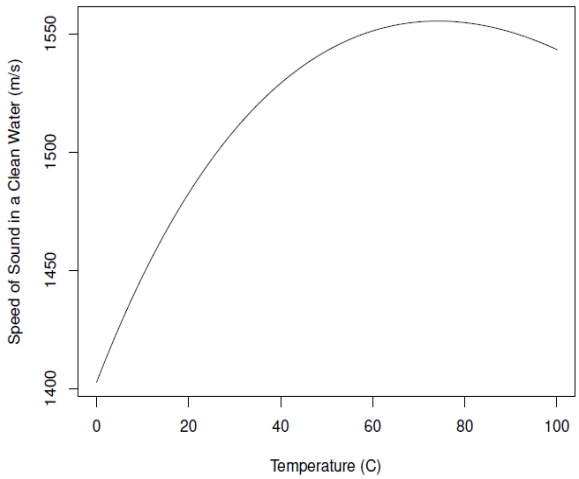

Fig. 2. The speed of sound in the clean water at various temperature

B. Calibration Techniques

Almost all types of flow meter requires its own calibration procedure due to the fluid flow process shows uncertain behaviors. Common sources of uncertainty under flow classified into two groups, such as random nature of the process and the system-based variations. Flow instability, not having perfectly homogeneous fluid (randomness); temperature variations along the flow path, pressure changes (system-based) are the most important parameters affect the results of the measurement [14-16].

One of the solutions to improve the flow stability is that to follow the average flow rate rather than the instantaneous flow measurements.

$$F_{avg} = \frac{1}{N}\sum_{i=0}^{N-1} F_i$$

where F_i is the instantaneous flow reading, N is the number of consecutive readings.

Temperature changes along the flow path is the most significant parameter on the variations in measurement. The velocity characteristic of the sound wave in the water is depicted in Fig. 2. A comprehensive numerical scheme to estimate the velocity at a given temperature is presented as [2];

$$c = \sum_{i=0}^{5} a_i T^i$$

where $a_0 = 1402.736$, $a_1 = 5.03358$, $a_2 = -0.0579506$, $a_3 = 0.000331636$, $a_4 = -1.45262E-06$, $a_5 = 0.30449E-08$ It is reported that 1 ^{o}C change in temperature may result in 0.05% variation in the volumetric flow rate. Hence, the calibration coefficient is updated as [18-20];

$$K(T) = \frac{K_{cal}}{1 + 3\alpha(T - T_{cal})}$$

where K_{cal} := calibration factor, T_{cal} := calibration temperature; T := actual temperature, α := linear thermal expansion coefficient taken as $69 \times 10^{-6}/C$.

Linear Least Squares, LLS

Let consider to have n joint measurements (observations) of x and y to build a mathematical model using the parameters β_0 and β_1, such that;

$$\begin{aligned} y_1 &= \beta_0 + \beta_1 x_1 + r_1 \\ y_2 &= \beta_0 + \beta_1 x_2 + r_2 \\ &\dots \\ y_n &= \beta_0 + \beta_1 x_n + r_n \end{aligned} \quad (8)$$

where r_i is the residuals (error) terms, β_0 is the intercept of the line with the $y-axis$, and β_1 is the slope of the line. The least squares approach is employed in order to determine the parameters to obtain the "best" fitting line in (8). The corresponding cost function is defined as;

$$h(\beta_0,\beta_1) = \frac{1}{2}\sum_{i=1}^{n} r_i^2 = \frac{1}{2}\sum_{i=1}^{n}(y_i - (\beta_0 + \beta_1 x_i))^2 \quad (9)$$

which subject to minimized. The partial derivatives of $h(\beta_0,\beta_1)$ with respect to β_0 and β_1 equal to zero at where the cost function, $h(\beta_0,\beta_1)$, is at its minimum.

$$\begin{aligned} \frac{\partial h(\beta_0,\beta_1)}{\partial \beta_0} &= \sum_{i=1}^{n}(y_i - (\beta_0 + \beta_1 x_i))(-1) \\ &= -\sum_{i=1}^{n} y_i + \beta_1 \sum_{i=1}^{n} x_i + n\beta_0 \\ \frac{\partial h(\beta_0,\beta_1)}{\partial \beta_1} &= \sum_{i=1}^{n}(y_i - (\beta_0 + \beta_1 x_i))(-x_i) \\ &= -\sum_{i=1}^{n} x_i y_i + \beta_1 \sum_{i=1}^{n} x_i^2 + \beta_0 \sum_{i=1}^{n} x_i \end{aligned} \quad (10)$$

Solutions of (10) supply the sample intercept and the sample slope denoted as $\hat{\beta}_0$, and $\hat{\beta}_1$, respectively;

$$\begin{aligned} \hat{\beta}_1 &= \frac{\sum_{i=1}^{n}(x_i-\bar{x})(y_i-\bar{y})}{\sum_{i=1}^{n}(x_i-\bar{x})^2} \\ \hat{\beta}_0 &= \bar{y} - \hat{\beta}_1 \bar{x} \end{aligned} \quad (11)$$

where $\bar{x}$ and $\bar{y}$ are the means of x and y;

$$\bar{x} = \frac{1}{n}\sum_{i=1}^{n} x_i$$

$$\bar{y} = \frac{1}{n}\sum_{i=1}^{n} y_i$$

Equation 11 can be written in an another form using some basic statistical definitions;

$$\boxed{\begin{aligned} \hat{\beta}_1 &= \frac{\sum_{i=1}^{n}(x_i-\bar{x})(y_i-\bar{y})}{\sum_{i=1}^{n}(x_i-\bar{x})^2} \\ \hat{\beta}_0 &= \bar{y} - \hat{\beta}_1 \bar{x} \end{aligned}} \quad (12)$$

$$\begin{aligned} \hat{\beta}_1 &= \frac{\hat{\sigma}_{xy}}{\hat{\sigma}_x^2} \\ \hat{\beta}_0 &= \bar{y} - \hat{\beta}_1 \bar{x} \end{aligned} \quad (13)$$

where $\hat{\sigma}_{xy}$ is the covariance between x and y, $\hat{\sigma}_{x^2}$ is the variance of x expressed as;

$$\hat{\sigma}_x^2 = \frac{1}{n-1}\sum_{i=1}^{n}(x_i-\bar{x})^2$$

$$\hat{\sigma}_{xy} = \frac{1}{n-1}\sum_{i=1}^{n}(x_i-\bar{x})(y_i-\bar{y})$$

The mathematical model of the regression line is given as;

$$\hat{y}_i = \hat{\beta}_0 + \hat{\beta}_1 x_i \quad (14)$$

In a general case, multi-variable (let p-variables linear regression model can be defined as;

$$\begin{bmatrix} y_1 \\ y_2 \\ \vdots \\ y_n \end{bmatrix}_{n\times 1} = \begin{bmatrix} 1 & x_{11} & \cdots & x_{1(p+1)} \\ 1 & x_{21} & \cdots & x_{2(p+1)} \\ \vdots & \cdots & \cdots & \vdots \\ 1 & x_{n1} & \cdots & x_{n(p+1)} \end{bmatrix}_{n\times(p+1)} \begin{bmatrix} \beta_0 \\ \beta_1 \\ \vdots \\ \beta_p \end{bmatrix}_{(p+1)\times 1} + \begin{bmatrix} r_1 \\ r_2 \\ \vdots \\ r_n \end{bmatrix}_{n\times 1} \quad (15)$$

In a simple notations;

$$\mathbf{Y} = \mathbf{X}\boldsymbol{\beta} + \mathbf{R} \quad (16)$$

$$\begin{bmatrix} y_1 \\ y_2 \\ \vdots \\ y_n \end{bmatrix} = \begin{bmatrix} 1 & x_{11} & \cdot & x_{1(p+1)} \\ 1 & x_{21} & \cdot & x_{2(p+1)} \\ \cdot & \cdot & \cdot & \cdot \\ 1 & x_{n1} & \cdot & x_{n(p+1)} \end{bmatrix} \begin{pmatrix} 1 & 0 \\ 0 & 1 \end{pmatrix} \begin{pmatrix} c \\ s \end{pmatrix} = c^2 + s^2 \quad (17)$$

Parameter Estimations

The objective of the parameter prediction is to minimize the cost function of;

$$h(\mathbf{R}) = \frac{1}{2}\sum_{i=1}^{n} r_i^2 = \frac{1}{2}\mathbf{R}^T\mathbf{R} \quad (18)$$

where $[.]^T$ is the transpose of the matrix $[.]^T$. Please note that;

$$\mathbf{R}^T\mathbf{R} = \begin{bmatrix} r_1 & r_2 & \dots & r_n \end{bmatrix} \begin{bmatrix} r_1 \\ r_2 \\ \vdots \\ r_n \end{bmatrix} = [r_1^2 + r_2^2 + \cdots + r_n^2]$$

using (16) $\mathbf{R}$ consisting of residuals can be expressed as;

$$\mathbf{R} = \mathbf{Y} - \mathbf{X}\boldsymbol{\beta}$$

then;

$$\begin{aligned} h(\mathbf{R}) &= \frac{1}{2}(\mathbf{Y}-\mathbf{X}\boldsymbol{\beta})^T(\mathbf{Y}-\mathbf{X}\boldsymbol{\beta}) \\ &= \frac{1}{2}\mathbf{Y}^T\mathbf{Y} - 2\boldsymbol{\beta}^T\mathbf{X}^T\mathbf{Y} + \boldsymbol{\beta}^T\mathbf{X}^T\mathbf{X}\boldsymbol{\beta} \end{aligned} \quad (19)$$

$\hat{\boldsymbol{\beta}}$ which minimizes the cost function, can be derived as i) derivation of (18) equals zero; ii) the second derivative of (18) must be positive. The first and the second derivatives of $h(\mathbf{R})$ with respect to $\hat{\boldsymbol{\beta}}$ are;

$$\begin{aligned} \frac{\partial h(\hat{\boldsymbol{\beta}})}{\partial \boldsymbol{\beta}} &= -\mathbf{X}^T\mathbf{Y} + \mathbf{X}^T\mathbf{X}\boldsymbol{\beta} = 0 \\ \frac{\partial^2 h(\hat{\boldsymbol{\beta}})}{\partial \boldsymbol{\beta}^2} &= \mathbf{X}^T\mathbf{X} > 0 \end{aligned} \quad (20)$$

As long as $\mathbf{X}$ is positive definite matrix, $\hat{\boldsymbol{\beta}}$ satisfied the condition being positive. The estimation of $\hat{\boldsymbol{\beta}}$ is derived from (20);

$$\hat{\boldsymbol{\beta}} = (\mathbf{X}^T\mathbf{X})^{-1}\mathbf{X}^T\mathbf{Y} \quad (21)$$

Weighted Linear Least Squares, WLS

In WLS the residuals are assumed to have different variances and an appropriate weighted matrix accompanying with the parameter estimation.

$$\hat{\boldsymbol{\beta}} = (\mathbf{X}^T\mathbf{W}\mathbf{X})^{-1}\mathbf{X}^T\mathbf{W}\mathbf{Y} \quad (22)$$

where

$$\mathbf{W} = \begin{bmatrix} w_1 & 0 & \dots & 0 \\ 0 & w_2 & \dots & 0 \\ \vdots & \vdots & \ddots & \vdots \\ 0 & 0 & \dots & w_n \end{bmatrix}$$

It is assumed that the errors occur only in the response (Y) data, not in the predictor (X) data. If the error shows a Gaussian random behavior, i.e. $\epsilon \sim \mathbf{N}(0, \sigma^2)$, the entries of $\mathbf{W}$ are expressed as;

$$w_i = \frac{1}{\sigma_i^2}$$

Piecewise Linear Least Squares, PLR

The characteristics of flow meter may change at various fluid flow levels. PLR allows us to develop a model based on combinations of multiple linear models. Assume that the data (x_i, y_i), $i = 1, \ldots, N$ with $x_i, y_i \in R$, and let $p_0, p_1, \ldots, p_k$ be knot points. The typical structure of a univariate PLR model can be defined as;

$$f(x) = \alpha_i x + \beta_i \quad (23)$$

where $x \in [p_{i-1}, p_i]$. Equation 23 must satisfy the following constraints;

- Convexity property $:= \alpha_1 < \alpha_2 < \cdots < \alpha_k$
- Continuity property $:= \alpha_i p_i + \beta_i = \alpha_{i+1} p_i + \beta_{i+1}$

Thereafter, the optimization problem turns into;

$$\text{minimize} \sum_{i=1}^{N} (f(x_i) - y_i)^2$$

$$\text{subject to}$$

$$\alpha_1 < \alpha_2 < \cdots \alpha_k$$

$$\alpha_i p_i + \beta_i = \alpha_{i+1} p_i + \beta_{i+1}$$

III. RESULT AND DISCUSSION

In this section, three common calibration methods, which have been discussed in Section 2, are employed to the data obtained from DN-20 type ultrasonic water flow meter. Various numbers of measurement have been carried out at 13 different water flow levels, and then averages of the measurements have been considered as measured data corresponding to the reference flow rate obtained by means of an electromagnetic flow meter. The results obtained from LLS, WLS, and PLR calibration methods are presented in Table 1.

Table 1 Results obtained from LLS, WLS, and PLR

		LLS		WLS		PLR	
Standard (L/h)	Reading (L/h)	Calibrated (L/h)	Error %	Calibrated (L/h)	Error %	Calibrated (L/h)	Error %
16	9.79	16.98	-6.11	16.91	-5.70	16.10	-0.65
25	17.27	25.86	-3.43	26.02	-4.08	24.77	0.91
40	29.33	41.47	-3.67	41.81	-4.53	39.56	1.09
60	45.88	61.08	-1.79	60.65	-1.08	60.50	-0.83
80	62.70	82.67	-3.34	81.20	-1.50	81.51	-1.88
120	99.23	122.10	-1.75	120.34	-0.28	121.79	-1.49
200	172.67	203.57	-1.79	199.01	0.50	204.63	-2.31
400	356.86	401.51	-0.38	396.34	0.92	405.22	-1.30
1000	911.99	1002.31	-0.23	991.06	0.89	1011.40	-1.14
1400	1280.38	1401.46	-0.10	1385.72	1.02	1415.68	-1.12
2800	2592.23	2818.43	-0.66	2791.13	0.32	2827.12	-0.97
4000	3719.61	4048.22	-1.21	3998.91	0.03	4048.69	-1.22
5000	4664.93	5072.75	-1.45	5011.65	-0.23	5060.33	-1.21

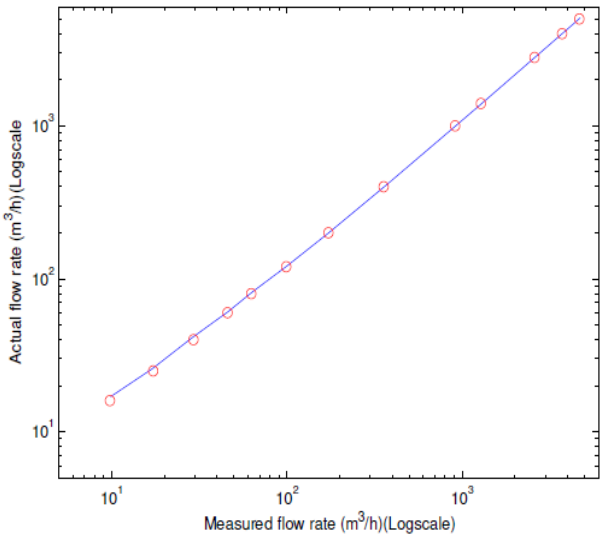

Fig. 3. Linear least squares approach

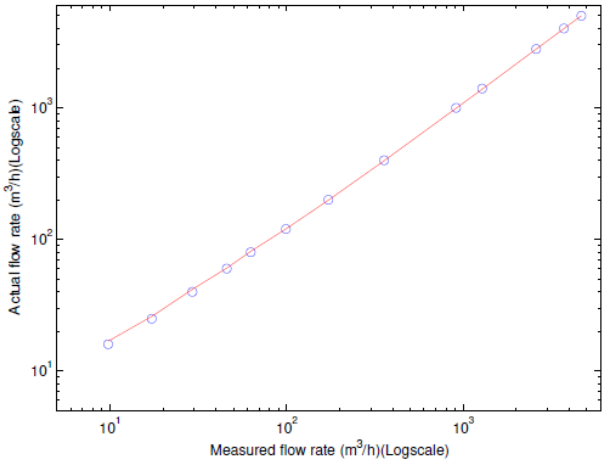

Fig. 4 Weighted Linear least squares approach

The calibrated results are depicted in Figures 3, 4, 5 achieved by LLS, WLS, and PLR, respectively. The percentage errors are illustrated in Figures 6, 7, 8. Considering the errors, PLR supplies the best results at over all case, while WLS is the best for the higher flow rates. Both WLS and LLS are especially not adequate for the low level of flow rates.

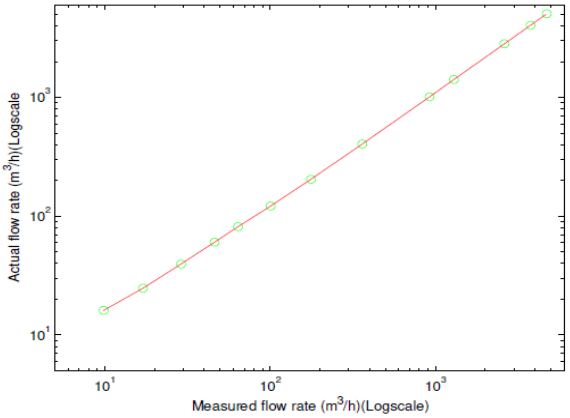

Fig. 5. Piecewise linear least squares approach

Fine Calibration

Fine calibration is considered as a necessary stage to avoid measuring errors due to the installation and environmental effects, possible fluctuations of variables temperature, density, viscosity, and pressure [19]. A handheld mobile terminal is proposed to carry out fine calibration operations. The terminal and the flow meter communicate via 434 MHz RF band. The main processes are illustrated in Figure 9 and Figure 10 for the flow meter side the terminal side, respectively. The less precisely calibrated flow meters are chosen in order to observe the efficacy of the fine calibration. The process can be outlined as;

1. Select calibration menu
2. Enter the meter no
3. Insert flow rates and corresponding errors (maximum at 12 separate data sets)
4. Microprocessor calculates the new calibration coefficients and do updates
5. RF transmits the flow and error data sets.

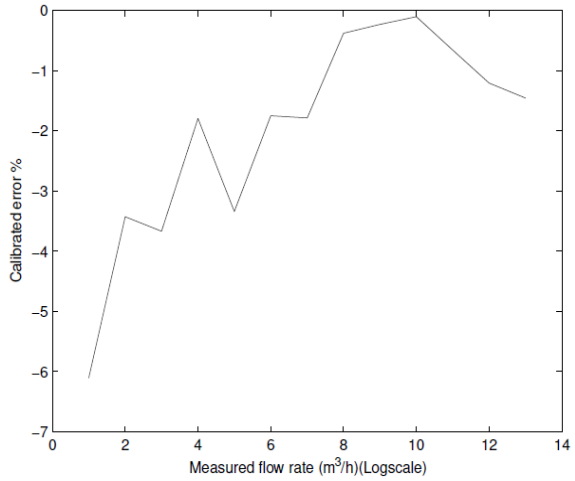

Fig. 6. Percentage error based on linear least squares approach

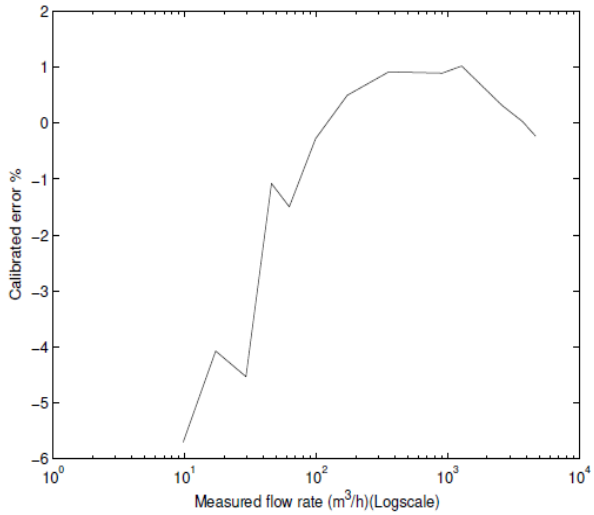

Fig. 7. Percentage error based on weighted linear least squares approach

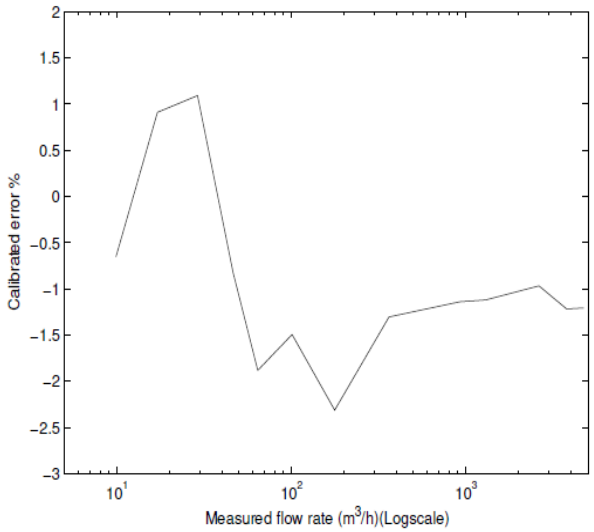

Fig. 8. Percentage error based on piecewise linear least squares approach

Table 2 Results of the fine calibration process

			Meter No			
		Flow rate (lt/h)	7	8	9	10
Error %	Before calibration	10	8.02	7.06	7.54	5.15
		40	3.56	5.57	2.55	6.58
		400	2.08	1.30	1.74	2.46
		900	2.42	4.06	4.26	-2.59
		2500	0.12	-0.25	-0.29	1.92
		3125	-4.18	-4.99	-7.67	-11.00
Error %	After calibration	10	-0.32	-0.83	-1.33	0.18
		40	1.10	1.10	1.61	1.61
		400	-0.13	0.26	-0.03	0.16
		900	0.14	-0.28	-0.08	0.31
		2500	-0.16	0.08	0.05	-0.37
		3125	-0.20	-0.73	-0.42	0.93

The results of the fine calibration procedure at various flow rates are shown in Table 2. According to the results, the percentage errors, which are out of acceptable error band, at various flow rates were reduced to the acceptable error band level.

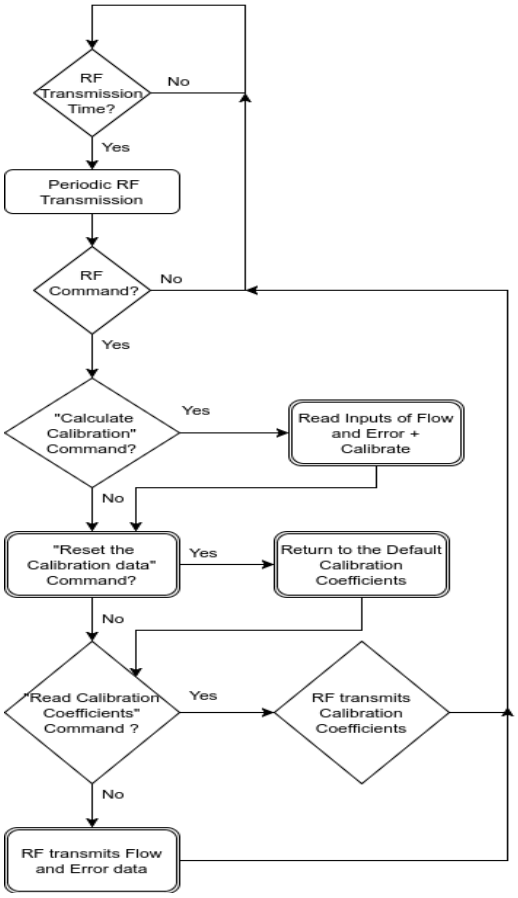

Fig. 9. Flowchart of the fine calibration at the flow meter side

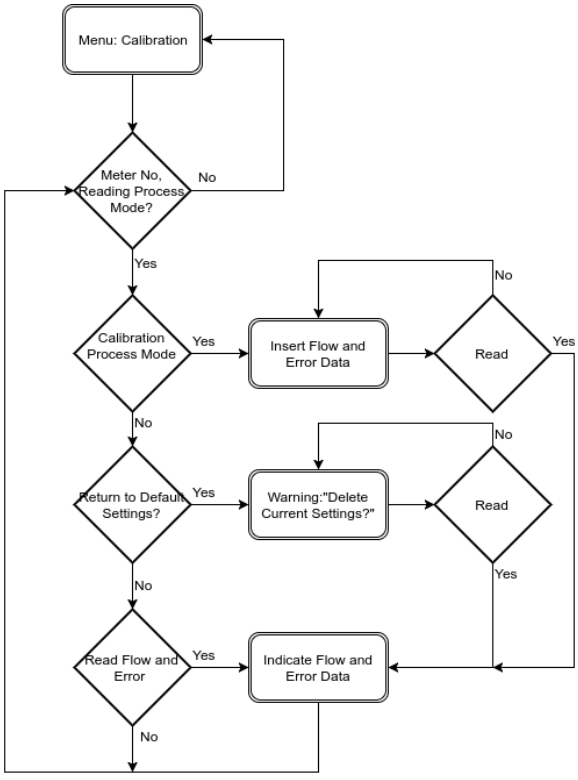

Fig. 10. Flowchart of the fine calibration at the terminal side

The results of the fine calibration procedure at various flow rates are shown in Table 2. According to the results, the percentage errors, which are out of acceptable error band, at various flow rates were reduced to the acceptable error band level.

IV. CONCLUSION

Reading of flow meters in a high precision has directly influence both on the domestic and on the industrial applications. Hence, calibration is an essential instance in order to get amendable and controllable measurements. In this study, three different calibration methods, namely, LLS, WLS, and PLR, were employed to calibrate an ultrasonic water flow meter. Although, LLS and WLS are sufficient at high flow rates based on percentage errors, PLR provides the best results at overall at overall performance. In addition, a handheld wireless terminal is efficient in order to fine calibration process.

REFERENCES

1. Rajita, G., & Mandal, N. (2016). Review on transit time ultrasonic flowmeter. In Control, Instrumentation, Energy & Communication (CIEC), 2016 2nd International Conference on (pp. 88–92). IEEE. DOI: https://doi.org/10.1109/ciec.2016.7513740
2. Greenspan, M. 1957. Speed of sound in water by a direct method. *J. Res. Natl. Bur. Stand.*, *59*, 249–254. DOI: https://doi.org/10.6028/jres.059.028
3. Yeh, T. T., Espina, P. I., & Osella, S. A. 2001, May. An intelligent ultrasonic flowmeter for improved flow measurement and flow calibration facility. In IMTC 2001. Proceedings of the 18th IEEE Instrumentation and Measurement Technology Conference. Rediscovering Measurement in the Age of Informatics (Cat. No. 01CH 37188) (Vol. 3, pp. 1741-1746). IEEE. DOI: https://doi.org/10.1109/imtc.2001.929499
4. Yazdanshenasshad, B., & Safizadeh, M. S. 2018. Neural-network-based error reduction in calibrating utility ultrasonic flow meters. Flow Measurement and Instrumentation, 64, 54-63. DOI: https://doi.org/10.1016/j.flowmeasinst.2018.10.003
5. Wang, Z., Andiroglu, E., Wang, G., & Song, L. 2019. Accuracy improvement of virtual pump water flow meters using calibrated characteristics curves at various frequencies. Energy and Buildings, 191, 143-150. DOI: https://doi.org/10.1016/j.enbuild.2019.03.021
6. Prettyman, J. B., Johnson, M. C., & Barfuss, S. L. 2016. Comparison of Selected Differential-Producing, Ultrasonic, and Magnetic Flow Meters. Journal-American Water Works Association, 108(1), E39-E49. DOI: https://doi.org/10.5942/jawwa.2016.108.0002
7. Hogendoorn, J., Hofstede, H., van Brakel, P., & Boer, A. 2011. How accurate are ultrasonic flowmeters in practical conditions; beyond the calibration. In 29th International north sea flow measurement workshop. 25–28.
8. Morita, R., Uchiyama, Y., Umezawa, S., & Sugita, K. 2018. Flow rate measurement of wet steam in small bore piping by clamp-on type ultrasonic flow meter. in The Proceedings of the National Symposium on Power and Energy Systems DOI: https://doi.org/10.1299/jsmepes.2018.23.d133
9. Pimenta, B. D., Robaina, A. D., Peiter, M. X., Kirchner, J. H., Mezzomo, W., & Torres, R. R. 2018. Performance of ultrasonic flow meter in different vinyl polychloride pipes. IRRIGA, 23(1), 87-95. DOI: https://doi.org/10.15809/irriga.2018v23n2p359-379
10. Peng, S., Liao, W., & Tan, H. 2018. Performance optimization of ultrasonic flow meter based on computational fluid dynamics. Advances in Mechanical Engineering, 10(8), 1687814018793264. DOI: https://doi.org/10.1177/1687814018793264
11. BIPM. (2012). International Vocabulary of Metrology.

12. Shourcheh, S. D., & Rezazadeh, G. 2016, October. Mechanical analysis of ultrasonic flow meter based on Doppler effect. In 2016 4th International Conference on Robotics and Mechatronics (ICROM) (pp. 14-19). IEEE. DOI: https://doi.org/10.1109/icrom.2016.7886778
13. Muramatsu, E., Murakawa, H., Hashiguchi, D., Sugimoto, K., Asano, H., Wada, S., & Furuichi, N. 2018. Applicability of hybrid ultrasonic flow meter for widerange flowrate under distorted velocity profile conditions. Experimental Thermal and Fluid Science, 94, 49-58. DOI:https://doi.org/10.1016/j.expthermflusci.2018.01.032
14. Upadhye, V., & Agashe, S. 2016. Effect of Temperature and Pressure Variations on the Resonant Frequency of Piezoelectric Material. Measurement and Control, 49(9), 286–292.
15. Mu, L. B., Xu, K. J., Liu, B., Tian, L., & Liang, L. P. 2019. Echo signal envelope fitting based signal processing methods for ultrasonic gas flow-meter. ISA transactions, 89, 233-244. DOI: https://doi.org/10.1016/j.isatra.2018.12.035
16. Leontidis, V., Cuvier, C., Caignaert, G., Dupont, P., Roussette, O., Fammery, S., ... & Dazin, A. 2018. Experimental validation of an ultrasonic flowmeter for unsteady flows. Measurement Science and Technology, 29(4), 045303. DOI: https://doi.org/10.1088/1361-6501/aaa65f
17. Choudhary, K. P., Arumuru, V., & Bhumkar, Y. G. 2019. Numerical simulation of beam drift effect in ultrasonic flow-meter. Measurement, 146, 705-717. DOI: https://doi.org/10.1016/j.measurement.2019.06.044
18. Tawackolian, K., Büker, O., Hogendoorn, J., & Lederer, T. 2013. Calibration of an ultrasonic flow meter for hot water. Flow Measurement and Instrumentation, 30, 166-173. DOI:https://doi.org/10.1016/j.flowmeasinst.2012.05.003
19. Dutta, P., & Kumar, A. 2017. Intelligent calibration technique using optimized fuzzy logic controller for ultrasonic flow sensor. Mathematical Modelling of Engineering Problems, 4(2), 91-94. DOI: https://doi.org/10.18280/mmep.040205
20. Sinha, S., Mandal, N., & Bera, S. C. 2016, January. Calibration of electrode polarization impedance type flow meter using neural network. In 2016 2nd International Conference on Control, Instrumentation, Energy & Communication (CIEC) (pp. 64-67). IEEE. DOI: https://doi.org/10.1109/ciec.2016.7513807
21. Pursley, W. C. 1986. The calibration of flowmeters. *Measurement and Control*, *19*(5), 37–45. DOI: https://doi.org/10.1177/002029408601900504

AUTHORS PROFILE

Muammer Catak received his BSc in Electrical and Electronics Engineering a from the Middle East Technical University, Turkey in 2004, the MSc in Telecommunication and Signal Processing, Blekinge Technical Institute, Sweden, the Ph.D. in Stochastic Modelling and Simulation from Process Engineering, University College Cork, Ireland in 2010. He is currently an Assistant Professorat the American University of the Middle East, Kuwait. His research interests includestochastic signal processing and industrial applications.

Coskun Ergan currently works as a software engineer at Baylan Measurement Intruments, Izmir, Turkey.